Available online at www.sciencedirect.com
SCIENCE DIRECT®
DNA Repair 4 (2005) 419–431
DNA REPAIR
www.elsevier.com/locate/dnarepair

The murine DNA glycosylase NEIL2 (mNEIL2) and human DNA polymerase β bind microtubules in situ and in vitro

Kimberly A. Conlon[a], Holly Miller[a,b], Thomas A. Rosenquist[a], Dmitry O. Zharkov[c], Miguel Berrios[a,d,*]

[a] *Department of Pharmacological Sciences, School of Medicine University Hospital and Medical Center, State University of New York Stony Brook, NY 11794 8651, USA*
[b] *Laboratory of Chemical Biology, University Hospital and Medical Center, State University of New York Stony Brook, NY 11794 8651, USA*
[c] *Novosibirsk Institute of Chemical Biology and Fundamental Medicine, 8 Lavrentieva Avenue, Novosibirsk 630090, Russia*
[d] *University Microscopy Imaging Center, State University of New York Stony Brook, NY 11794 8088, USA*

Received 20 September 2004; accepted 29 October 2004
Available online 18 January 2005

Abstract

8-Oxoguanine DNA glycosylase (OGG1), a major DNA repair enzyme in mammalian cells and a component of the base excision repair (BER) pathway, was recently shown to be associated with the microtubule network and the centriole at interphase and the spindle assembly at mitosis. In this study, we determined whether other participants in the BER pathway also bind microtubules in situ and in vitro. Purified recombinant human DNA polymerase β (DNA Pol β) and purified recombinant mNEIL2 were chemically conjugated to fluorochromes and photosensitive dyes and used in in situ localization and binding experiments. Results from in situ localization, microtubule co-precipitation and site-directed photochemical experiments showed that recombinant human DNA Pol β and recombinant mNEIL2 associated with microtubules in situ and in vitro in a manner similar to that shown earlier for another BER pathway component, OGG1. Observations reported in this study suggest that these BER pathway components are microtubule-associated proteins (MAPs) themselves or utilize yet to be identified MAPs to bind microtubules in order to regulate their intracellular trafficking and activities during the cell cycle.

Keywords: BER; DNA repair; Microtubules; MAPs; DNA Pol β; NEIL2

1. Introduction

Reactive oxygen species (ROS) have been linked to aging and the onset of several disorders ranging from cancer to Alzheimer's disease [1–5]. Endogenous ROS formation increases when cells are exposed to environmental pollutants [6,7], certain drugs [8], nutrient deprivation [9] oxidizing agents or ionizing radiation [10–12] and during some pathological processes such as inflammation or ischemia–reperfusion [13]. Although cellular anti-oxidant defenses (e.g., catalase, peroxidase, superoxide dismutase) can effectively combat the effects of ROS, oxidative DNA damage still occurs. ROS-induced lesions involve several base modifications in either free nucleotides or DNA including a relatively stable oxidized form of guanine: 7,8-dihydro-8-oxoguanine (8-oxoG) [14,15].

Except for double strand breaks, oxidative DNA damage is repaired primarily through the BER pathway [16]. The BER pathway has multiple enzymatic steps initiated with the excision of oxidatively damaged bases by one of several DNA glycosylases [16,17]. In higher eukaryotes, after the participation of glycosylases, DNA repair is completed by an abasic site endonuclease, DNA polymerase (DNA Pol β) combining deoxyribose phosphate lyase and DNA polymerase activities, and a DNA ligase [16,18]. Until recently,

* Corresponding author. Tel.: +1 631 4443050; fax: +1 631 4443218.
E-mail address: miguel@pharm.sunysb.edu (M. Berrios).

1568-7864/$ – see front matter © 2004 Elsevier B.V. All rights reserved.
doi:10.1016/j.dnarep.2004.10.010

only two mammalian DNA glycosylases capable of repairing oxidized base lesions had been described, NTH1 and OGG1 [19]. Enzymatically, NTH1 and OGG1 are considered *Escherichia coli N*th-type glycosylases since their active sites contain a helix–hairpin–helix motif and a proline/glycine loop motif, which define the NTH superfamily of DNA repair proteins [17]. It is known however, that *E. coli* has two other DNA glycosylases capable of excising oxidized DNA bases named MutM and Nei. Enzymatically, MutM and Nei are different from NTH1 and OGG1 in that they utilize an N-terminal proline residue in their active site to carry-out βδ elimination to generate a 3′-phosphate group at the DNA cleavage site and have an N-terminal PE-motif, helix–two-turn–helix motif, and zinc finger motifs instead of the NTH-specific motifs [20,21]. In 2002, Hazra and colleagues identified two human orthologs of *E. coli* MutM and Nei naming them Nei homologs NEH1 and NEH2 (later re-named NEIL1 and NEIL2, respectively [22,23]). Recently, Rosenquist and colleagues purified and enzymatically characterized the bacterially-expressed recombinant murine NEIL1 (mNEIL1) showing that this gene product was a DNA glycosylase that excised both cis-thymine glycol diastereoisomers as well as the formamidopyrimidine derivatives of guanine (G) and adenine (A) in irradiated DNA [24]. Enzymatic characterization of the recombinant NEIL2 protein confirmed that this gene product was a DNA glycosylase/lyase using an N-terminal proline residue in its active site to perform βδ elimination on DNA abasic sites [17,23]. In addition, it was shown that NEIL2 differs enzymatically from NEIL1 in that NEIL2 has a substrate preference for ROS-oxidized cytosine [23].

Although extensive information has been accumulated on the substrate specificity of the BER pathway participants, there is less information about regulation of their intracellular trafficking and activities. Antibodies directed against human OGG1 (hOGG1) or another DNA glycosylase hMYH (the human homolog for bacterial MutY, a mismatched adenine-DNA glycosylase) localized these enzymes to mitochondria and nuclei of human cells [25,26]. Takao and collaborators using transiently expressed epitope-tagged hOGG1, hMYH and the human homolog of NTH1 (hNTH1) showed that these enzymes were localized mostly to the nucleus and mitochondria in simian Cos7 cells [27]. Using a stable transfectant cell line expressing GFP-tagged hOGG1, it was shown that hOGG1 was preferentially associated with a nuclear matrix or karyoskeleton-enriched fraction and chromatin during interphase and became associated with mitotic chromosomes at mitosis [28]. Based on these observations, it is now accepted that there are distinct nuclear and cytoplasmic pools of OGG1, with the former composed of a single isoform, OGG1-1a, and the latter, of several isoforms lacking the nuclear localization signal [27,29]. Furthermore, transfectant cells transiently expressing epitope-tagged NEIL2 revealed that this enzyme is found both in the nucleus and cytoplasm of these cells [22]. DNA Pol β, a key player in the BER pathway, that replaces the excised base and deoxyribose sugar with the correct nucleotide, has been immunocytochemically localized to mitochondria and nuclei in parasitic protozoa [30,31], to nuclei in chicken cells [32] and to somatic nuclei and meiotic chromosomes in mammalian cells [33,34].

We previously reported that cytoplasmic pools of murine OGG1 (mOGG1) redistribute to the nucleus and nuclear periphery in response to nutrient deprivation and oxidative DNA damage [9]. This redistribution suggested that intracellular trafficking of mOGG1 may be mediated, in part, by active transport. This observation together with a previous report showing the association of OGG1 with the nuclear matrix or karyoskeleton [28], suggested that a similar relationship to that observed with the karyoskeleton may also exist between DNA repair proteins and the cytoskeleton.

The cytoskeleton is a filamentous network spanning the cytoplasm and composed of three major cytoskeletal polymers: actin filaments, intermediate filaments and microtubules. These filaments interact with each other and with many different associated proteins to mediate the trafficking of macromolecules and small organelles through the cytoplasm [17,35–38]. The apparent universality of this trafficking is substantiated by the wide range of macromolecules transported by the cytoskeleton. For example, cells use microtubules to regulate the trafficking of mRNAs and cofactors from transcription and processing sites in the nucleus to translation and degradation sites in the cytosol [39,40]. MAPs are major components of the cytoskeleton [41,42]. MAPs can be classified into three groups: structural MAPs (or microtubule interactive proteins (MIPs)), movement-related MAPs (or motor proteins) and unconventional MAPs [43]. Besides serving other functions, microtubules themselves or in conjunction with MAPs, transport macromolecules (i.e. mRNAs and proteins) to or from the nuclear periphery and throughout the cytoplasm [44,45]. Microtubule binding facilitates not only the bidirectional trafficking of macromolecules but also prevents their dilution and allows for regulation of their activity by targeting them to a cell compartment (e.g., the nucleus) where their activity is needed [40]. The redistribution of proteins and their functional control is exemplified by the recent discovery that tumor suppressors, among other DNA regulatory proteins, traffic over microtubule networks using movement-related MAPs [46,47].

There is accumulating evidence indicating that microtubules are involved in the regulation of DNA synthesis and its repair. For instance, centrosomes, in addition to participating in the organization of the spindle assembly at mitosis, have been shown to play a critical role in cell cycle progression, chromosome stability and cellular responses to DNA replication defects and DNA damage [48–50]. Over expression of DNA Pol β, a common phenomenon in several human cancers [51,52] has been associated with centrosome defects at mitosis and chromosome instability [49,52–54]. Tumor suppressor proteins, including APC and p53, also have been shown to use microtubules for intracellular trafficking [46,55].

The mechanism of action of most chemotherapeutic agents is known; many target the structure and metabolism of DNA and RNA either directly or indirectly while others target microtubule stability. Despite recent advances there are still large gaps in our knowledge, particularly on how exposure to chemotherapeutic agents triggers apoptosis and cell death. Microtubule-disrupting drugs act by interfering with microtubules' dynamic stability and by blocking cells in mitosis. As such these drugs are among the most widespread chemotherapeutic agents. It is conceivable that microtubule-disrupting drugs' effectiveness in inducing apoptosis and cell death may be in part derived from their capacity to disrupt intracellular transport in general and of key enzymes in DNA metabolism, including those involved in DNA repair, in particular.

Recent evidence from our laboratory demonstrated that hOGG1 and mOGG1 bind microtubules during interphase and mitosis lending further support to the hypothesis that the cytoskeleton, in particular microtubules, play an important role in the distribution of DNA repair enzymes during interphase and mitosis [56]. In light of this recent evidence, we have addressed the possibility that other participants in the BER pathway, specifically DNA Pol β and mNEIL2, also bind microtubules in vitro and in situ. We chose these BER pathway participants because they differ from OGG1 in that DNA pol β has no glycosylase activity and, although NEIL2 is also a glycosylase/lyase, it belongs to a different superfamily of DNA repair proteins and is enzymatically different from OGG1. Results from this study showed that purified recombinant human DNA Pol β and purified recombinant mNEIL2 associate with microtubules in vitro and in situ in a manner similar to that shown earlier for OGG1 isoforms.

2. Materials and methods

2.1. Materials

Actin, bovine serum albumin (BSA), Coomassie blue, dithiothreitol (DTT), formamide, ethylenediaminetetraacetic acid (EDTA), iodoacetamide (IAA), isopropyl β-D-thiogalactopyranoside (IPTG), 2-mercaptoethanol, dimethylsulfoxide (DMSO), phenylsulfonyl chloride (PMSF), polyethylenimine, 1-4-piperazinediethanesulfonic acid (Pipes), *N*-[hydroxyethyl] piperazine-*N*′-[2-ethanesulfonic acid] (HEPES), bisbenzimide (H 33258), paclitaxel (taxol), lysozyme, aprotinin, antipain, pepstatin A, DNase I and trypsin (from bovine pancreas) were purchased from Sigma Chemical Co. (St. Louis, MO). GTP, dNTPs and leupeptin were purchased from Boehringer Mannheim Biochemicals (Indianapolis, IN). Mammalian tubulin (from bovine brain) was purchased from Cytoskeleton, Inc. (Denver, CO). Paraformaldehyde, Triton X-100, [ethylenebis(oxyethylenenitrilo)] tetraacetic acid (EGTA) and urea were purchased from Fisher Scientific Co. (Springfield, NJ). Sodium dodecyl sulfate (SDS) was purchased from British Drug Houses (Poole, England). Bovine calf serum was purchased from HyClone (Logan, UT). Dulbecco's Modified Eagle's Medium (DMEM), penicillin G, streptomycin, kanamycin, chlorophenicol and L-glutamine were purchased from Invitrogen (Grand Island, NY). Acrylamide, *N*,*N*′-methylene-bisacrylamide and *N*,*N*,*N*′,*N*′-tetramethylethylenediamine were purchased from Eastman Kodak Co. (Rochester, NY). EMDSO3 was purchased from Merck Chemicals Ltd. (Poole, UK). Hitrap Heparin Sepharose and S-Sepharose were purchased from Pharmacia (Uppsala, Sweden). POROS SP column chromatography matrix was purchased from IBA, GmbH (Gottingen, Germany). Bccmount was purchased from BCC Microimaging (Stony Brook, NY). All other chemicals were obtained commercially, were of reagent grade, and were used without further purification.

2.2. Antibodies

FITC-conjugated mouse anti-α tubulin monoclonal antibodies and mouse anti-γ tubulin monoclonal antibodies were purchased from Sigma Chemical Co. (St. Louis, MO). Rabbit anti-mOGG1 antiserum directed against the whole wild-type recombinant mOGG1 polypeptide was as previously described [57]. Rabbit anti-human DNA Pol β antibodies (Ab-3, PB-1674-P1) were purchased from Lab Vision (Fremont, CA). Rabbit anti-mNEIL2 antibodies were produced in collaboration with Cocalico Biologicals (Reamstown, PA) by injection of C-terminal hexahistidine-tagged full-length mNEIL2 protein. Affinity goat anti-rabbit IgG (H&L chains) conjugated to Alexa 488 antibodies were purchased from Molecular Probes (Eugene, OR).

2.3. Cloning, expression and purification of human DNA Pol β

Cloning was as previously described [58]. Briefly, the cDNA of human DNA Pol β was cloned into a λ P_L promoter-based bacterial expression system. Recombinant protein was purified as a polypeptide containing 334 residues starting with Ser2 due to the removal of an N-terminus methionine during bacterial expression [59]. Expression of human DNA Pol β was a modification of previously described protocols [58,59]. Briefly, when *E. coli* media reached an OD_{600} of 1.0 they were induced for 2 h at 42 °C. Cells were resuspended in TED buffer (1 mM EDTA, 1 mM DTT, 50 mM Tris–Cl, pH 8.0) supplemented with 50 mg/ml lysozyme, 10 mM $Na_2S_2O_5$, 500 mM NaCl, 1 mg/ml pepstatin A and 1 mM PMSF. After sonication the clarified supernatant was resuspended in 60% (w/v) ammonium sulfate, the precipitate removed and the supernatant brought to 85% (w/v) ammonium sulfate. The protein precipitate 85% (w/v) ammonium sulfate was solubilized in TED and DNA Pol β purified to homogeneity after consecutive fractionation through Fractogel $EMDSO_3$, POROS SP and Hitrap Heparin Sepharose column chromatography.

2.4. Cloning, expression and purification of mNEIL2

Cloning of mNEIL2 cDNA into expression plasmid pET24b was as previously described for mouse NEIL1 [24]. Briefly, mNEIL2 cDNA was cloned into the expression plasmid using primers to yield a native mNEIL2 protein when expressed lacking a hexahistidine C-terminal tag. *E. coli* BL21(DE3)-RIL (pET24b /mNeil2) were grown at 37 °C in 1 L of 2xYT medium containing 25 μg/ml kanamycin and 25 μg/ml chlorophenicol. When the culture media OD_{600} reached 0.6–0.8, $ZnCl_2$ and IPTG were added to a final concentration of 10 μM and 0.2 mM, respectively. After 3 h incubation, cells were harvested by low speed centrifugation at 4 °C and stored at −80 °C (3–4 g of wet weight). Frozen cells were thawed and resuspended in 50 ml of triethanolamine buffer pH 8.0, supplemented with 1 mM PMSF. Lysozyme and DNase I were added to a final concentration of 100 and 1 μg/ml, respectively. After incubation at room temperature for 20 min, NaCl (final concentration 1 M) was added and the cell suspension was stirred for 30 min on ice. Cell lysates were cleared by centrifugation at 25,000 × *g* for 30 min at 4 °C. The supernatant was treated with 100 μl of 5% (v/v) polyethylenimine solution and the centrifugation step repeated. Proteins were precipitated from the supernatant by addition of ammonium sulfate at 50% (w/v) saturation.

After 2 h incubation on ice, the protein precipitate was centrifuged at 25,000 × *g* for 20 min at 4 °C. The resulting pellet was dissolved in buffer A (1 mM EDTA, 1 mM DTT, 20 mM HEPES, pH 7.5) supplemented with 200 mM NaCl and loaded onto a 70 ml S-Sepharose column equilibrated with buffer A supplemented with 200 mM NaCl. Proteins were eluted using 400 ml of a 200–800 mM NaCl gradient in buffer A. Fractions containing mNEIL2 were pooled, diluted with buffer A to 200 mM NaCl and loaded in portions (10–12 mg of protein) onto 5 ml HiTrap Heparin Sepharose column. Proteins were eluted with 20 column volumes of a 200–600 mM NaCl linear gradient in buffer A. The peak fractions were diluted two-fold with buffer A and adsorbed onto a SP/F 10/100 POROS SP column. MNEIL2 was eluted using 20 column volumes of a 200–600 mM NaCl linear gradient in buffer A. Protein fractions were analyzed by SDS-PAGE. Fractions with at least 95% pure protein were pooled, dialyzed against the storage buffer (400 mM NaCl, 1 mM EDTA, 1 mM DTT, 50% (v/v) glycerol, 50 mM HEPES, pH 7.5) and stored at −20 °C until use.

2.5. Conjugation of recombinant DNA Pol β and mNEIL2 to the N-hydroxysuccinimide (NHS) esters of rhodamine and Rose Bengal hexanoic acid (RBHA)

Chemical conjugation of DNA Pol β and mNEIL2 to the NHS esters of rhodamine (rhodamine-NHS) and RBHA (RBHA-NHS) was as follows: 50 μl containing 3.5 mg/ml purified recombinant DNA Pol β or 20 μl containing 3.5 mg/ml purified recombinant mNEIL2 was dialyzed overnight at 4 °C against 20 ml of a solution containing 250 mM NaCl; 50% (v/v) glycerol; 50 mM $NaHCO_3$, pH 9.0. After dialysis, reaction mixtures received either 1 μg of rhodamine-NHS or 2 μg of RBHA-NHS in DMSO before they were incubated for 1 h at room temperature on a Roto-Shake Genie (Scientific Industries, Bohemia, NY). After incubation, reaction mixtures were dialyzed overnight at 4 °C against 20 ml of a solution containing 250 mM NaCl; 50% (v/v) glycerol; 50 mM Tris–Cl, pH 8.2. Dye conjugates were stored at −20 °C until use.

2.6. Tissue culture

NIH 3T3 cells (Swiss mouse embryo fibroblasts) were obtained from the American Type Culture Collection (Manassas, VA) and kept frozen in liquid nitrogen until use as previously described [56]. Briefly, NIH 3T3 fibroblasts were thawed and cultured in DMEM, supplemented with 10% (v/v) calf serum, 2 mM L-glutamine, 0.1 mM non-essential amino acids, 1 mM sodium pyruvate and 100 IU/ml penicillin G, 100 μg/ml streptomycin. Unless specified otherwise NIH 3T3 fibroblasts were plated onto glass microscope slides in 10 cm tissue culture dishes at a density of 2 to 5×10^5 cells/dish for DNA Pol β and mNEIL2 binding studies, in situ photochemistry and indirect immunofluorescence staining [57,60]. To enrich for cells in mitosis, cells growing on microscope slides and culture media containing free (floater) cells were mounted onto a Cytobucket (IEC, Needham Heights, MA) customized to fit two-well immunofluorescent chambers (EMS, Hatfield, PA) and centrifuged at 400 × *g* for 40 min in a Centra-CL3 Series centrifuge (Thermo IEC, Needham Heights, MA). After centrifugation, the media was removed and cells fixed with paraformaldehyde essentially as described for immunofluorescence microscopy.

2.7. Decoration of microtubules by fluorescently-tagged DNA Pol β or fluorescently-tagged mNEIL2

Decoration of network and mitotic assembly microtubules with rhodamine-conjugated DNA Pol β or rhodamine-conjugated mNEIL2 was performed using two-well immunofluorescence chambers (EMS, Hatfield, PA) as previously described [56]. Procedures were conducted at room temperature unless specified. Briefly, cells were fixed with paraformaldehyde, washed with MSM-Pipes and incubated for 15 min at 37 °C with a freshly prepared 200 μl solution containing 3 μg rhodamine-conjugated DNA Pol β or 660 ng rhodamine-conjugated mNEIL2. After incubation, cells were rinsed three times with MSM-Pipes and mounted with glass coverslips using 4 μl of Bccmount.

2.8. Cell lysis

To prepare fractions enriched in MAPs, tubulin and other cellular proteins, actively growing NIH 3T3 fibroblasts were placed on ice and harvested by centrifugation at 2000 × *g* for 10 min. Cells were washed free of media by resuspension in

ice-cold PBS (140 mM NaCl; 10 mM phosphate buffer pH 7.4) followed by centrifugation at 2000 × *g* for 10 min. The final cell pellet was resuspended in an equal volume of ice-cold PEM buffer (1 mM MgSO; 2 mM EGTA; 100 mM Pipes, pH 6.9) supplemented with 10% (v/v) glycerol and aprotinin, antipain, leupeptin and pepstatin A (1 μg/ml each). Complete cell lysis was achieved by brief sonication on ice (4–5 pulses #6 setting, W185 Sonifier Cell Disruptor, Plainview, NY). Cell lysis was monitored by phase contrast microscopy. Cell lysates were cleared by centrifugation at 12,200 × *g* for 10 min and supernatants centrifuged again in the same manner before being aliquoted and kept at −20 °C until use.

2.9. SDS-PAGE

SDS-PAGE was as previously described [56,61]. Briefly, proteins were solubilized in boiling sample loading buffer [2% (w/v) SDS; 10% (v/v) glycerol; 20 mM DTT; 2 μg/ml bromophenol blue; 62.5 mM Tris–Cl pH 6.8] and boiled for 5 min. Alkylation of thiol groups on proteins was performed by incubating supernatants in the presence of 20 mM IAA for 30 min at room temperature in the dark. SDS-PAGE gel-separated proteins were visualized using Coomassie blue. Gels were stained overnight.

2.10. Polymerization of tubulin into taxol-stabilized microtubules

Microtubules were assembled in vitro from tubulin-enriched fractions as previously described [43]. Briefly, lyophilized bovine brain tubulin was resolubilized in PEM buffer supplemented with 10% (v/v) glycerol and the protease inhibitors aprotinin, antipain, leupeptin and pepstatin A (1 μg/ml each), and its concentration adjusted to 5 mg/ml. 1 mM Mg^{2+}GTP was added and the mixture incubated in a water bath at 37 °C for 30 min. After incubation, taxol was added to a final concentration of 20 μM and the mixture incubated in a water bath at 37 °C for 5 min.

Microtubule polymerization was monitored by phase contrast microscopy. The concentration of taxol-stabilized microtubules was adjusted to 4 mg/ml with PEM buffer supplemented with 10% (v/v) glycerol, 20 μM taxol and the protease inhibitors aprotinin, antipain, leupeptin and pepstatin A (1 μg/ml each) before being aliquoted and stored at 4 °C until use. Under these conditions taxol-stabilized microtubules were stable for about a week.

2.11. Microtubule binding and co-precipitation of DNA Pol β and mNEIL2

In vitro assembled taxol-stabilized microtubules were incubated in the presence of either purified recombinant mOGG1 (control), or DNA Pol β or mNEIL2 and microtubule-complexes formed precipitated by centrifugation as described [62,63]. The co-precipitation assay was conducted as follows: briefly, 30 μl of a mixture containing 130 μg/ml taxol-stabilized microtubules in PEM buffer supplemented with 10% (v/v) glycerol, 2 mg/ml Mg^{2+}GTP, 20 μg/ml taxol in the presence or absence of MAP-enriched cell lysates (20%, v/v) were mixed with either recombinant mOGG1 (control) or DNA Pol β or mNEIL2 and incubated for 15 min at 37 °C. To conduct microtubule-binding experiments under conditions in which the amount of microtubules was not a limiting factor, the concentration of taxol-stabilized microtubules in the incubation mixture was increased to 3.3 mg/ml instead of 130 μg/ml (a 25-fold increase). Microtubule stability was monitored by phase contrast microscopy. After incubation, microtubules were precipitated by centrifugation at room temperature under conditions that do not precipitate soluble proteins including tubulin subunits (15 min at 12,200 × *g*). Proteins in pellets (precipitated microtubules) and those contained in two-third volume of each supernatant were solubilized in boiling SDS-PAGE loading buffer and analyzed by SDS-PAGE.

2.12. In situ site-directed photochemistry

In situ photochemistry was performed essentially as previously described [56]. Briefly, NIH 3T3 fibroblasts were grown on heat-sterilized but otherwise untreated glass microscope slides at a concentration of 45 cells/mm^2. Incubation with Rose Bengal-conjugated DNA Pol β (RB-DNA Pol β) or Rose Bengal-conjugated mNEIL2 (RB-mNEIL2) and irradiation with visible light were conducted in two-well immunofluorescence chambers (EMS, Hatfield, PA) as follows: slides were mounted into immunofluorescence chambers, fixed with paraformaldehyde and cells washed free of culture media with fresh MSM-Pipes. MSM-Pipes contained 18 mM $MgSO_4$; 5 mM $CaCl_2$; 41 mM KCl; 24 mM NaCl; 0.5% (v/v) Triton X-100; 0.5% (v/v) of either Tween 20 or Nonidet P40; 5 mM Pipes, pH 7.5 [64]. To each well, 200 μl containing 0.6 μg of RB-DNA Pol β or 1.8 μg of RB-mNEIL2 in MSM-Pipes were added. Control wells received either 200 μl of unconjugated RB-DNA Pol β or unconjugated RB-mNEIL2 diluted 1:200 in MSM-Pipes. Mixtures containing either RB-DNA Pol β or RB-mNEIL2 were incubated in the dark for 15 min at 37 °C using a humidified chamber. After incubation, cells were washed once with 400 μl of MSM-Pipes. After washings, 800 μl of MSM-Pipes were added, and cells were irradiated for 60 min at 37 °C with visible light. Visible light irradiation conditions were as previously described [56].

2.13. In vitro site-directed photochemistry

In vitro site-directed photochemical digestion of tubulin subunits was as previously described [56] with the following modifications. Briefly, taxol-stabilized microtubules were prepared as described above. Reaction mixtures (10 μl) containing 0.4 mg/ml taxol-stabilized microtubules in PEM buffer supplemented with 10% (v/v) glycerol, 2 mM Mg^{2+}GTP, and 20 μM taxol were placed into clear borosil-

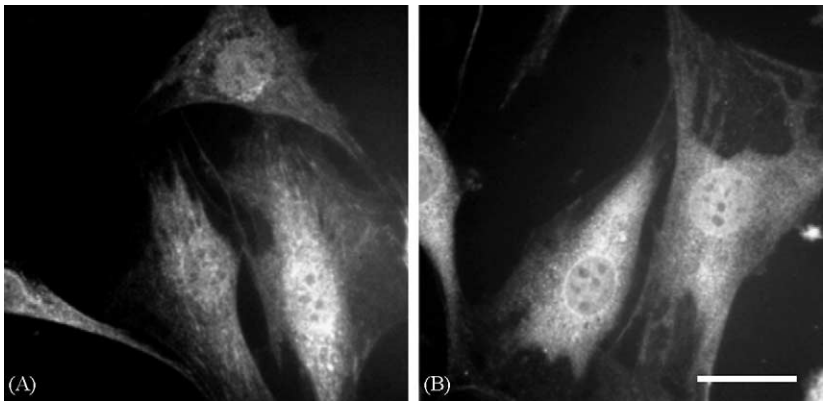

Fig. 1. Immunofluorescent staining of NIH 3T3 fibroblasts with antibodies directed against either human DNA Pol β or mNEIL2. Indirect immunofluorescence was performed as described in Section 2. (A and B) Epifluorescent micrographs. (A) Cells probed with rabbit anti-DNA Pol β antibodies followed by Alexa 488-conjugated goat anti-rabbit IgG antibodies. (B) Cells probed with rabbit anti-mNEIL2 antibodies followed by Alexa 488-conjugated goat anti-rabbit IgG antibodies. (B) Bar, 25 μm applies to both panels.

icate glass tubes. To each reaction mixture either 1.2 μg of RB-mOGG1 (control), or 1.2 μg of RB-DNA Pol β, or 1.2 μg of RB-mNEIL2 was added. Control mixtures containing RB-conjugates were incubated in the dark at 37 °C for 15 min. Visible light irradiation conditions were as previously described [61]. After irradiation, protein digestion products were solubilized in boiling SDS-PAGE loading buffer and analyzed by SDS-PAGE.

2.14. Fluorescence and immunofluorescence microscopy

Cell fixation with paraformaldehyde and fluorescent and indirect immunofluorescent staining were as previously described [56,64]. Cells were fixed at room temperature to preserve microtubules. Briefly, after probing cells with fluorochrome-tagged probes, cells were mounted under a glass coverslip with 4 μl of Bccmount. Specimens were examined with a 40×/0.75 planachromat phase objective lens using an Axiophot epifluorescent photomicroscope (Carl Zeiss, Jena, Germany). Wide-field micrographs were acquired using MaxIm DL/CCD image acquisition and processing software package (Diffraction Ltd., Ottawa, Canada) with a KX14E (A3156) cooled CCD camera system (Apogee Instruments, Auburn, CA) attached to the video port of the above photomicroscope.

3. Results

3.1. Indirect immunofluorescence microscopy reveals that DNA Pol β and mNEIL2 are localized to the nucleus and the peripheral cytoplasm of mouse tissue culture cells

Rabbit antibodies directed against two BER pathway components, DNA Pol β or mNEIL2, were used as specific probes to localize the authentic enzymes in mouse fibroblasts by indirect immunofluorescence microscopy. Results from these experiments are shown in Fig. 1. Indirect immunofluorescence analyses were conducted as described in Section 2. To eliminate the possibility of fluorescent signal bleed through, no fluorescent dyes for nucleic acids (DNA) or mitochondria were used. Cell nuclei and their nucleoli were identified using phase contrast microscopy (not shown). Immunofluorescence microscopy revealed that DNA Pol β and mNEIL2 were localized to the nuclear interior and the cytoplasm of NIH 3T3 fibroblasts (Fig. 1A and B). Nuclear staining with anti-DNA Pol β or anti-mNEIL2 antibodies showed a diffuse pattern that excluded areas occupied by nucleoli (Fig. 1A and B). Cytoplasmic staining with anti-DNA Pol β or anti-mNEIL2 antibodies showed a punctate pattern that was concentrated around the nuclear periphery (Fig. 1A and B). A fibrillar-like staining pattern that seemed organized along strands or filaments was observed elsewhere in the cytoplasm with anti-DNA Pol β or anti-mNEIL2 antibodies (Fig. 1A and B). When indirect immunofluorescence was conducted using either non-specific antibodies or omitting the first specific antibodies (controls) no staining was observed (not shown).

We recently reported that the human and murine OGG1 proteins (isoform 1a) bind the microtubule network and the centrosome (centriole) of interphase cells and the spindle assembly at mitosis [56]. This observation lent further support to the notion that the cytoskeleton, in particular microtubules, may play an important role in the distribution of DNA repair enzymes during interphase and mitosis [56]. In light of this recent evidence, it was important to determine whether other participants in the BER pathway, specifically human DNA Pol β and mNEIL2, also bind microtubules assembled in vitro and tubulin assemblies in mammalian tissue culture cells. To test this hypothesis, purified recombinant human DNA Pol β and purified recombinant mNEIL2 were chemically conjugated to a fluorochrome (rhodamine) and to the photo-reactive dye Rose Bengal (RB). Chemical conjugation of the dyes rhodamine and RB to either recombinant human DNA Pol β or recombinant mNEIL2 was as described in Section 2. Chemical conjugation was confirmed by TLC.

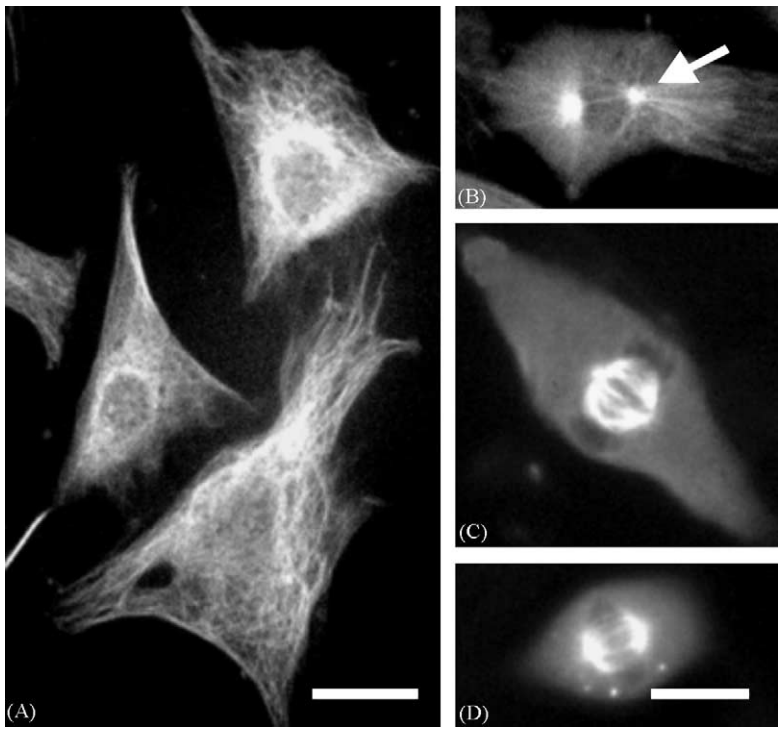

Fig. 2. Decoration of the microtubule network at interphase and the spindle assembly at mitosis by fluorescently-tagged recombinant DNA Pol β. Chemical conjugation of recombinant DNA Pol β to rhodamine and cell probing with rhodamine-conjugated DNA pol β was as described in Section 2. (A–D) Epifluorescent micrographs of NIH 3T3 fibroblasts probed with rhodamine-conjugated DNA Pol β. (A) Interphase cells. (B–D) Cells entering or during mitosis. (B) Prophase. Arrow points to one of the forming spindle assembly poles. (C) Metaphase. (D) Anaphase. (A) Bar, 25 μm. (D) Bar, 20 μm.

3.2. Fluorescently-tagged DNA Pol β and fluorescently-tagged mNEIL2 decorate the microtubule network and centrosome at interphase and the spindle assembly at mitosis

Once the fluorescent dye rhodamine was conjugated to recombinant human DNA Pol β and mNEIL2, these fluorescently-tagged proteins were used to probe freshly fixed NIH 3T3 fibroblasts. Results from these in situ localization experiments are shown in Figs. 2 and 3. Fluorescently-tagged DNA Pol β decorated an extensive network of microtubules emanating from or near the centrosome of interphase cells (Fig. 2A and B). At mitosis, however, fluorescently-tagged DNA Pol β decorated microtubules forming the spindle assembly (Fig. 2C and D). The centrioles, at the centrosome and at the spindle assembly poles, were evidenced by immunofluorescent staining with anti-γ tubulin antibodies (not shown). The microtubule network at interphase and the mitotic spindle assembly were evidenced by immunofluorescent staining with anti-α tubulin antibodies as described in Section 2 (not shown). Fluorescently-tagged DNA Pol β also showed a diffuse staining, not associated with microtubules, in interphasic and mitotic cells (Fig. 2A–D). This diffuse staining was largely excluded from the nuclear interior (not shown) and the space occupied by metaphase chromosomes, however (Fig. 2C). The nucleus and the space occupied by metaphase chromosomes were evidenced by phase contrast microscopy and fluorescent staining with DNA-specific dyes (not shown). Similar results to those obtained with fluorescently-tagged DNA Pol β were obtained when NIH 3T3 fibroblasts were probed with fluorescently-tagged mNEIL2 (Fig. 3). Fluorescently-tagged mNEIL2 also decorated the microtubule network of interphasic NIH 3T3 fibroblasts (Fig. 3A and B). Microtubule decoration by fluorescently-tagged mNEIL2 was most prominent near the cell's centrosome (Fig. 3A and B (arrows)). At mitosis, fluorescently-tagged mNEIL2 decorated the spindle assembly (Fig. 3C and D). Like the staining pattern obtained with fluorescently-tagged DNA Pol β (Fig. 2), fluorescently-tagged mNEIL2 also showed a diffuse staining pattern of the cytoplasm in interphase and mitotic cells (Fig. 3). Too, this diffuse staining was largely excluded from the nuclear interior (Fig. 3A and B) and the space occupied by metaphasic chromosomes (Fig. 3C) as evidenced by phase contrast microscopy (not shown). As reported previously [56], NIH 3T3 fibroblasts showed no staining when probed with fluorescently-tagged BSA (a non-specific probe) (not shown).

3.3. DNA Pol β and mNEIL2 bind in vitro and co-precipitate with taxol-stabilized microtubules

To determine whether DNA Pol β and mNEIL2 also bind to in vitro assembled microtubules, taxol-stabilized micro-

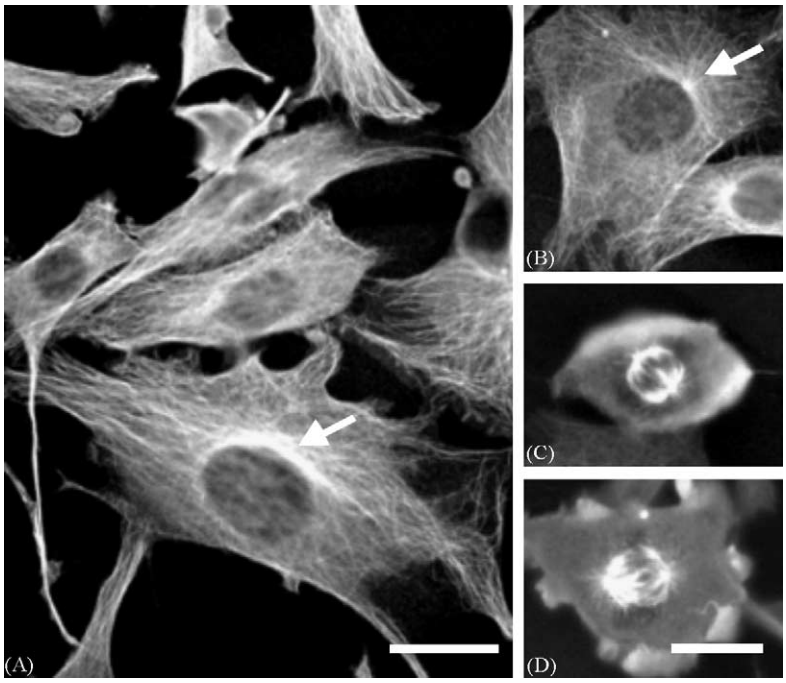

Fig. 3. Decoration of the microtubule network at interphase and the spindle assembly at mitosis by fluorescently-tagged recombinant mNEIL2. Chemical conjugation of recombinant mNEIL2 to rhodamine and cell probing with rhodamine-conjugated mNEIL2 was as described for Fig. 2. (A–D) Epifluorescent micrographs of NIH 3T3 fibroblasts probed with rhodamine-conjugated mNEIL2. (A and B) Interphase cells. Arrows point to the centrosome (centriole). (C and D) Cells in mitotic metaphase. (A) Bar, 25 μm applies to panels A and B. (D) Bar, 20 μm applies to panels C and D.

tubules were incubated in the presence of unmodified recombinant DNA Pol β or mNEIL2 either in the presence or the absence of tubulin- and MAP-enriched cell lysates. Microtubule polymerization from tubulin-enriched fractions, the preparation of tubulin/MAP-enriched cell lysates and microtubule co-precipitation assays were conducted as described in Section 2. The migration positions of mOGG1, DNA Pol β and mNEIL2 in this SDS-PAGE gel system were corroborated in blots by the corresponding specific antibodies. Results from these binding and co-precipitation experiments are shown in Fig. 4. DNA Pol β and mNEIL2 co-precipitated with taxol-stabilized microtubules (Fig. 4A, lanes 3 and 5, respectively). The co-precipitation of DNA Pol β and mNEIL2 with taxol-stabilized microtubules was apparently not altered by the presence of cell lysates enriched in tubulin, MAPs and other cellular proteins (Fig. 4B, lanes 3 and 5). The relative increase shown by the tubulin band in SDS-PAGE gel lanes containing cell lysates (Fig. 4B, lanes 1, 3 and 5) suggests that, during incubation, monomeric tubulin present in these lysates polymerized to extend existing taxol-stabilized microtubules and/or to form new microtubules. These additional microtubules, however, were not sufficient to precipitate all the DNA Pol β (and mOGG1) from incubation mixtures (Fig. 4B, lanes 4 and 2, respectively). Under the conditions of this assay, taxol-stabilized microtubules appear to be a limiting factor in co-precipitating of DNA Pol β and mNEIL2 from the incubation mixtures. In fact, quantitatively complete co-precipitation of DNA Pol β and mNEIL2 by taxol-stabilized microtubules was obtained by increasing up to 25-fold the concentration of taxol-stabilized microtubules (not shown).

3.4. Affinity binding and photo-digestion of in vitro-assembled-microtubule complexes by either Rose Bengal-tagged DNA Pol β or mNEIL2 confirm their association with tubulin assemblies

To confirm the binding specificity between DNA Pol β and mNEIL2 for taxol-stabilized microtubules and circumvent problems associated with chemical cross-linking analysis of relatively large macromolecular complexes (not shown), in vitro site-directed photo-digestion analyses of DNA Pol β and mNEIL2 microtubule complexes were performed. In vitro assembly of microtubules and in vitro site-directed photochemical experiments were conducted as described in Section 2. Results from these in vitro site-directed photochemical experiments are shown in Fig. 5. Reaction mixtures containing taxol-stabilized microtubules and either RB-mOGG1 (Fig. 5, lanes 1 and 2) or RB-DNA Pol β (Fig. 5, lanes 3 and 4) or RB-mNEIL2 (Fig. 5, lanes 5 and 6) were incubated in the absence (Fig. 5, lanes 1, 3 and 5) or the presence (Fig. 5, lanes 2, 4 and 6) of visible light. After irradiation, protein samples were analyzed by SDS-PAGE and protein bands identified by Coomassie blue staining. Tubulin migrated on SDS-PAGE gels at its expected mobility either in the presence or absence of visible light (Fig. 5, lanes 1, 3, 5 and lanes 2, 4, 6, respectively). However, SDS-PAGE gels showed that tubulin derived from taxol-stabilized microtubules was

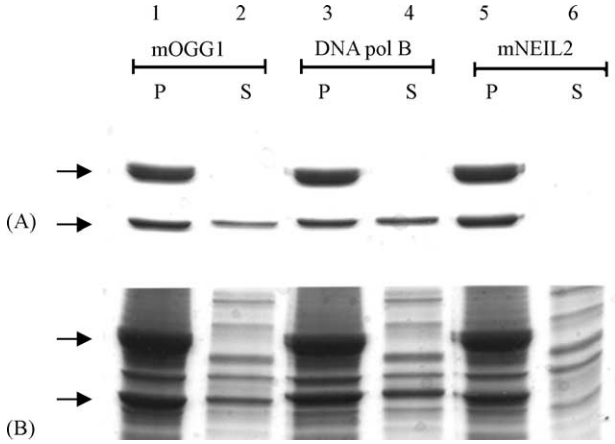

Fig. 4. Purified recombinant DNA Pol β and mNEIL2 co-precipitate with in vitro-assembled taxol-stabilized microtubules. Preparation of cell lysates, in vitro assembly of taxol-stabilized microtubules, microtubule co-precipitation assays and SDS-PAGE analyses were conducted as described in Section 2. (A) Coomassie blue stained 7.5–15% (w/v) SDS-polyacrylamide gradient gel containing proteins co-precipitated with (bound to) taxol-stabilized microtubules (P; pellet lanes) and their corresponding (unbound) supernatants (S; supernatant lanes) in the absence of MAP-enriched cell lysates and either mOGG1 (lanes 1 and 2), DNA Pol β (lanes 3 and 4) or mNEIL2 (lanes 5 and 6). (B) Coomassie blue stained 7.5–15% (w/v) SDS-polyacrylamide gradient gel containing proteins co-precipitated with (bound to) taxol-stabilized microtubules (P; pellet lanes) and their corresponding (unbound) supernatants (S; supernatant lanes) in the presence of MAP-enriched cell lysates and either mOGG1 (lanes 1 and 2), DNA Pol β (lanes 3 and 4) or mNEIL2 (lanes 5 and 6). (A and B) Arrows at left indicate the migration positions of α and β tubulin subunits (top arrows in each panel) and the approximate migration positions of mOGG1 (39-kDa), DNA Pol β (39-kDa) or mNEIL2 (39-kDa) (bottom arrows in each panel).

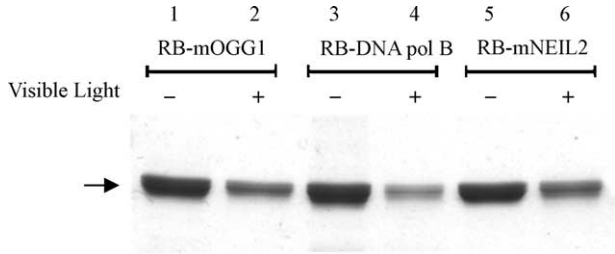

Fig. 5. In vitro site-directed photo-digestion of microtubule subunits by microtubule-bound RB-DNA Pol β and microtubule-bound RB-mNEIL2. In vitro site-directed photochemical digestion of tubulin subunits from taxol-stabilized microtubules by RB-mOGG1, RB-DNA Pol β or RB-mNEIL2 microtubule-bound complexes and SDS-PAGE were conducted as described in Section 2. RB-mOGG1, RB-DNA Pol β or RB-mNEIL2 bound to taxol-stabilized microtubules were incubated in the absence (lanes 1, 3 and 5) or in the presence (lanes 2, 4 and 6) of visible light and photo-digestion reactions analyzed by SDS-PAGE. Reaction mixtures were irradiated for 60 min at 37 °C. Each lane of a 7.5–15% (w/v) SDS-polyacrylamide gel was loaded with photo-digestion mixtures containing 0.4 mg/ml of taxol-stabilized microtubules and 1.2 μg of either RB-mOGG1, RB-DNA Pol β or RB-mNEIL2. SDS-PAGE gels were stained overnight with Coomassie blue. Lanes 1 and 2 show the tubulin band in reaction mixtures containing RB-mOGG1. Lanes 3 and 4 show the tubulin band in reaction mixtures containing RB-DNA Pol β. Lanes 5 and 6 show the tubulin band in reaction mixtures containing RB-mNEIL2. Arrow to the left, points to the migration position of α and β tubulin.

photo-digested in the presence of visible light and either RB-DNA Pol β (Fig. 5, lane 4) or RB-mNEIL2 (Fig. 5, lane 6). Similar photo-digestion was obtained with RB-mOGG1 (control, Fig. 5, lane 2). Tubulin photo-digestion was more prominent in RB-DNA Pol β-microtubule complexes than that observed with microtubule complexes formed by RB-mNEIL2 and RB-mOGG1 (control) under these experimental conditions. As reported previously [56], when actin (a non-specific protein) was added to incubation mixtures containing RB-conjugates it remained intact after irradiation with visible light (not shown).

3.5. Cells probed with RB-DNA Pol β or RB-mNEIL2 in the presence of visible light showed disruption of their microtubule networks

In situ site-directed photodigestion was previously used to evaluate protein–protein binding to elements of the cytoskeleton [56,57]. In this study, in situ site-directed protein photo-digestion was used to evaluate the disruption of microtubule network in RB-DNA Pol β and RB-mNEIL2-treated cells. Cell probing with RB-DNA Pol β and RB-mNEIL2 and in situ site-directed photochemistry was as described in Section 2. Results from these experiments are shown in Fig. 6. Cells probed with unmodified DNA Pol β or mNEIL2 in the presence of visible light (Fig. 6A and C, respectively) did not show detectable changes in their microtubule networks. Microtubules were disrupted, however, in cells probed with RB-DNA Pol β or RB-mNEIL2 in the presence of visible light (Fig. 6B and D). The microtubule network in these cells was not disrupted when these experiments were conducted in the absence of visible light (not shown).

4. Discussion

Studies focused on the BER pathway have been largely directed at characterizing their components and their enzymatic activities. The relatively few studies that have turned their attention to in situ localization have shown that BER pathway participants are distributed between the two major cell compartments, the nucleus and the cytoplasm [22,25–31,33,34]. Recently, however, recombinant mOGG1 tagged to fluorescent or photosensitive dye molecules was used to determine whether the cytoskeleton plays a role in the distribution of this specific BER pathway component. Results from these direct in situ localization studies showed that OGG1 binds microtubules, one of the three main protein polymers constituting the cell cytoskeleton [56]. Specifically, fluorescently-tagged mOGG1 decorated an extensive network of microtubules emanating from the centriole/centrosome at interphase and the spindle assembly at mitosis [56]. Furthermore, in situ localization observations were substantiated by results from chemical cross-linking and site-directed photo-digestion analyses [56].

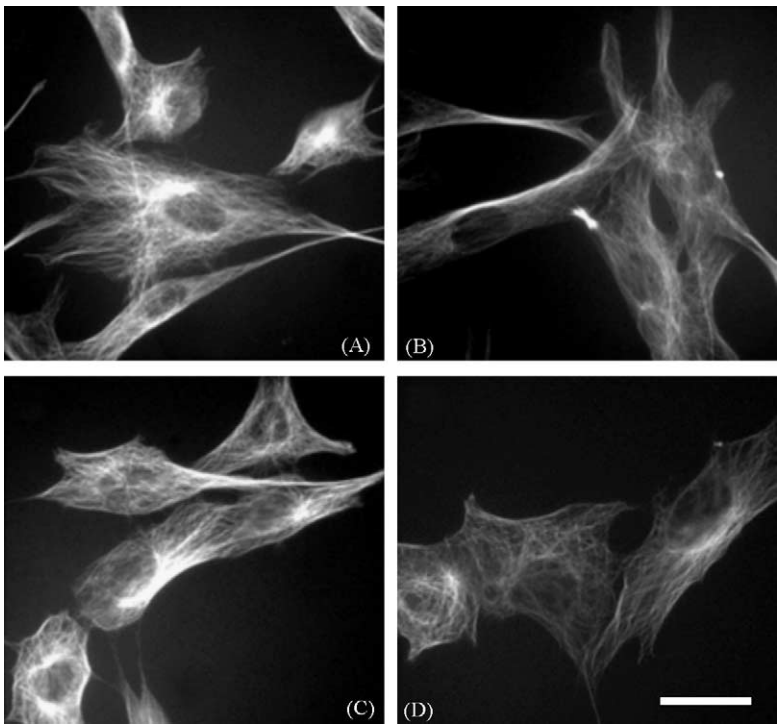

Fig. 6. In situ site-directed photo-disruption of the microtubule network by RB-DNA Pol β or RB-mNEIL2. NIH 3T3 fibroblasts were grown on slides, fixed with paraformaldehyde, washed with MSM-Pipes and incubated with either unconjugated DNA Pol β or NEIL2 or RB-DNA Pol β or RB-mNEIL2 in the presence of visible light as described in Section 2. Cells were irradiated with visible light for 60 min at 37 °C and microtubules decorated with FITC-conjugated mouse anti-tubulin monoclonal antibodies. (A–D) Epifluorescent micrographs. (A and B) Cells probed with unconjugated DNA Pol β and RB-DNA Pol β, respectively. (C and D) Cells probed with unconjugated mNEIL2 and RB-mNEIL2, respectively. (D) Bar, 25 μm applies to all panels.

The binding of OGG1 to microtubules, a cytoskeletal component involved in cellular trafficking, suggested that perhaps other members of the BER pathway may also use microtubules to reach cell compartments where their activity is needed (e.g., the nucleus). To substantiate this hypothesis and extend our previous observations with OGG1, we performed indirect immunofluorescent localization and direct localization studies in combination with binding and site-directed photochemical studies to determine whether human DNA Pol β and mNEIL2 also associate with microtubules in situ and in vitro. These BER pathway participants differ from OGG1 in that DNA Pol β has no glycosylase activity and, although NEIL2 is also a glycosylase/lyase, it is enzymatically and structurally different. In this study, using antibodies directed against DNA Pol β and mNEIL2 as well as fluorescently-tagged recombinant DNA Pol β and fluorescently-tagged recombinant mNEIL2 as specific probes, it was determined that these two enzymes in the BER pathway bind microtubules at interphase and mitosis. Immunofluorescent localization analyses confirmed the nuclear and cytoplasmic localization of DNA Pol β and mNEIL2. Cytoplasmic staining with anti-DNA Pol β and anti-mNEIL2 antibodies, seemed, at least in part, associated with filamentous material, a staining pattern that was reminiscent of previous observations with anti-mOGG1 antibodies in these same cells [57]. Furthermore, decoration of microtubules during the cell cycle by fluorescently-tagged DNA Pol β and mNEIL2 was similar to that observed previously with fluorescently-tagged OGG1 [56]. Fluorescently-tagged DNA Pol β and mNEIL2 also showed a diffuse staining pattern that largely excluded the space occupied by the nucleus and metaphasic chromosomes. This diffuse staining is consistent with the absence of microtubules in the nucleus of these cells, the presence of unbound DNA Pol β or NEIL2 and the microtubule's dynamic instability model [65] which proposes that monomeric tubulin pools exist in a dynamic, rather than a true equilibrium with tubulin assemblies [66,67]. Therefore, it is possible that DNA Pol β and mNEIL2 may be found as free cytosolic components as well as associated with tubulin molecules and smaller (growing) microtubules residing in the cytosol. In situ localization observations were corroborated by in situ site-directed photochemistry. Taken together these observations suggest that this dynamic equilibrium persists through the cell cycle keeping a fraction of cytoplasmic DNA Pol β and mNEIL2 pools associated with tubulin/microtubules. Using strategies that combined co-precipitation with taxol-stabilized microtubules and in vitro site-directed photo-protein digestion confirmed that recombinant human DNA Pol β and recombinant mNEIL2 also have an affinity for microtubules polymerized in vitro.

To our knowledge the association of DNA Pol β and mNEIL2 with tubulin assemblies has not been reported previously. Failure to observe this association may be explained by the detrimental effect of the in situ localization techniques

used on microtubule integrity and/or cell expression of tagged probe constructs themselves may have a lower affinity for or not bind microtubules in vivo. As suggested earlier, the fraction of DNA Pol β or mNEIL2 bound to microtubules may be relatively small with respect to enzyme pools found elsewhere in cells, thus, making it difficult to detect by immunofluorescence. Furthermore, microtubules are particularly susceptible to catastrophic collapse (e.g., cold, hydrostatic pressure, etc.). Any one of the above scenarios would preclude previous studies from detecting either DNA Pol β or mNEIL2-microtubule complexes in situ.

Although the association of DNA Pol β and mNEIL2 with microtubules cannot be ruled out as an artifact, this scenario seems unlikely since the murine and human homologs of OGG1 also demonstrated similar properties [56]. Furthermore, chemical conjugation to dye molecules and experimental manipulations during the conduction of these studies apparently did not alter DNA Pol β's or mNEIL2's capacity to bind microtubules. Too, DNA Pol β's and mNEIL2's capacity to bind microtubules seems to rule out the need for specific isoforms as suggested earlier for OGG1 [56]. The significance of splice variants may be related to targeting a specific destination/final site of action. Binding of hOGG1, mOGG1, mNEIL2 and human DNA Pol β to tubulin assemblies from different sources is also not surprising in light of the high homology found among microtubule proteins. Observations suggest that DNA Pol β's and mNEIL2's affinity for microtubules is relatively strong, thus, this stability may translate into a practical method for the affinity purification of these and other BER pathway components.

The observation that DNA Pol β and mNEIL2 bind to in vitro-assembled microtubules does not rule out the possibility that their interactions with microtubules may be regulated by posttranslation modifications and/or mediated through MAPs, however. Microtubules assembled in vitro from tubulin-enriched fractions or formed in the presence of cell lysates as described in this report, are not MAP-free tubulin assemblies. Proposals suggesting that MAPs may be forming bridges between DNA Pol β or NEIL2 and microtubules remain an open question and constitute an attractive model in light of the results presented here and elsewhere [56]. This type of MAP-mediated intracellular transport has already been shown to occur for other small macromolecules (proteins and nucleic acids), thus, it is possible that BER pathway enzymes are using MAPs riding on microtubules as a mechanism to regulate their activity while relocating in the cytoplasm and shuttling to the nucleus. Furthermore, microtubule-disrupting drugs are among the most effective anti-cancer chemotherapeutic agents and conceivably their effectiveness may be in part derived from their capacity to disrupt intracellular trafficking in general and of BER pathway enzymes in particular. The end result would be an increase in DNA damage and cell apoptosis. Studies are currently underway in our laboratory to test these and related hypotheses.

Acknowledgments

We wish to thank Wen Hui Feng, Rebecca Rowehl, LeeAnn Silver and Gregory Rudomen for expert technical assistance. We also wish to thank Konstantin Kropachev, Elena Zaika and Arthur Grollman for providing advice and samples of purified recombinant mOGG1 and mNEIL2. This work was supported by research grants CA8403301 from the National Cancer Institute (to M.B.), R29009113 from the National Institute of Environmental Health Sciences (to T.A.R.) and 02-04-49605 from the Russian Foundation for Basic Research and a fellowship from the Russian Science Support Foundation (to D.O.Z.).

References

[1] B.N. Ames, M.K. Shigenaga, T.M. Hagen, Oxidants, anti-oxidants, and the degenerative diseases of aging, Proc. Natl. Acad. Sci. U.S.A. 90 (1993) 7915–7922.
[2] D.C. Malins, R. Haimanot, Major alterations in the nucleotide structure of DNA in cancer of the female breast, Cancer Res. 51 (1991) 5430–5432.
[3] J.P. Spencer, A. Jenner, O.I. Aruoma, P.J. Evans, H. Kaur, D.T. Dexter, P. Jenner, A.J. Lees, D.C. Marsden, B. Halliwell, Intense oxidative DNA damage promoted by L-dopa and its metabolites: implications for neurodegenerative disease, FEBS Lett. 353 (1994) 246–250.
[4] Z.I. Alam, A. Jenner, S.E. Daniel, A.J. Lees, N. Cairns, C.D. Marsden, P. Jenner, B. Halliwell, Oxidative DNA damage in the parkinsonian brain: an apparent selective increase in 8-hydroxyguanine levels in *Substantia nigra*, J. Neurochem. 69 (1997) 1196–1203.
[5] M.A. Lovell, C. Xie, W.R. Markesbery, Decreased base excision repair and increased helicase activity in Alzheimer's disease brain, Brain Res. 855 (2000) 116–123.
[6] Y. Tsurudome, T. Hirano, H. Yamato, I. Tanaka, M. Sagai, H. Hirano, N. Nagata, H. Itoh, H. Kasai, Changes in levels of 8-hydroxyguanine in DNA, its repair and OGG1 mRNA in rat lungs after intratracheal administration of diesel exhaust particles, Carcinogenesis 20 (1999) 1573–1576.
[7] H.N. Kim, Y. Morimoto, T. Tsuda, Y. Ootsuyama, M. Hirohashi, T. Hirano, I. Tanaka, Y. Lim, I.G. Yun, H. Kasai, Changes in DNA 8-hydroxyguanine levels, 8-hydroxyguanine repair activity, and hOGG1 and hMTH1 mRNA expression in human lung alveolar epithelial cells induced by crocidolite asbestos, Carcinogenesis 22 (2001) 265–269.
[8] A. Kinoshita, H. Wanibuchi, S. Imaoka, M. Ogawa, C. Masuda, K. Morimura, Y. Funae, S. Fukushima, Formation of 8-hydroxydeoxy guano sine and cell-cycle arrest in the rat liver via generation of oxidative stress by phenobarbital: association with expression profiles of p21(WAF1/Cip1), cyclin D1 and OGG1, Carcinogenesis 23 (2002) 341–349.
[9] K.A. Conlon, A.P. Grollman, M. Berrios, Immunolocalization of 8-oxoguanine in nutrient-deprived mammalian tissue culture cells, J. Histotech. 23 (2000) 37–44.
[10] H. Kasai, H. Tanooka, S. Nishimura, Formation of 8-hydroxyguanine residues in DNA by X-irradiation, Gann 75 (1984) 1037–1039.
[11] H. Kasai, P.F. Crain, Y. Kuchino, S. Nishimura, A. Ootsuyama, H. Tanooka, Formation of 8-hydroxyguanine moiety in cellular DNA by agents producing oxygen radicals and evidence for its repair, Carcinogenesis 7 (1986) 1849–1851.
[12] J.L. Ravanat, J. Cadet, Reaction of singlet oxygen with 2′-deoxyguanosine and DNA. Isolation and characterization of the main oxidation products, Chem. Res. Toxicol. 8 (1995) 379–388.

[13] K. Tsuruya, M. Furuichi, Y. Tominaga, M. Shinozaki, M. Tokumoto, T. Yoshimitsu, K. Fukuda, H. Kanai, H. Hirakata, M. Iida, Y. Nakabeppu, Accumulation of 8-oxoguanine in the cellular DNA and the alteration of the OGG1 expression during ischemia–reperfusion injury in the rat kidney, DNA Rep. (Amst.) 2 (2003) 211–229.
[14] H. Kasai, S. Nishimura, DNA damage induced by asbestos in the presence of hydrogen peroxide, Gann 75 (1984) 841–844.
[15] A.P. Grollman, M. Moriya, Mutagenesis by 8-oxoguanine: an enemy within, Trends Genet. 9 (1993) 246–249.
[16] M. Christmann, M.T. Tomicic, W.P. Roos, B. Kaina, Mechanisms of human DNA repair: an update, Toxicology 193 (2003) 3–34.
[17] H. Ide, M. Kotera, Human DNA glycosylases involved in the repair of oxidatively damaged DNA, Biol. Pharm. Bull. 27 (2004) 480–485.
[18] T. Lindahl, Recognition and processing of damaged DNA, J. Cell Sci. Suppl. 19 (1995) 73–77.
[19] R. Lu, H.M. Nash, G.L. Verdine, A mammalian DNA repair enzyme that excises oxidatively damaged guanines maps to a locus frequently lost in lung cancer, Curr. Biol. 7 (1997) 397–407.
[20] D.O. Zharkov, R.A. Rieger, C.R. Iden, A.P. Grollman, NH2-terminal proline acts as a nucleophile in the glycosylase/AP-lyase reaction catalyzed by *Escherichia coli* formamidopyrimidine-DNA glycosylase (Fpg) protein, J. Biol. Chem. 272 (1997) 5335–5341.
[21] D. Jiang, Z. Hatahet, J.O. Blaisdell, R.J. Melamede, S.S. Wallace, *Escherichia coli* endonuclease VIII: cloning, sequencing, and overexpression of the nei structural gene and characterization of nei and nei *n*th mutants, J. Bacteriol. 179 (1997) 3773–3782.
[22] T.K. Hazra, Y.W. Kow, Z. Hatahet, B. Imhoff, I. Boldogh, S.K. Mokkapati, S. Mitra, T. Izumi, Identification and characterization of a novel human DNA glycosylase for repair of cytosine-derived lesions, J. Biol. Chem. 277 (2002) 30417–30420.
[23] T.K. Hazra, T. Izumi, I. Boldogh, B. Imhoff, Y.W. Kow, P. Jaruga, M. Dizdaroglu, S. Mitra, Identification and characterization of a human DNA glycosylase for repair of modified bases in oxidatively damaged DNA, Proc. Natl. Acad. Sci. U.S.A. 99 (2002) 3523–3528.
[24] T.A. Rosenquist, E. Zaika, A.S. Fernandes, D.O. Zharkov, H. Miller, A.P. Grollman, The novel DNA glycosylase, NEIL1, protects mammalian cells from radiation-mediated cell death, DNA Rep. (Amst.) 2 (2003) 581–591.
[25] I. Boldogh, D. Milligan, M.S. Lee, H. Bassett, R.S. Lloyd, A.K. McCullough, hMYH cell cycle-dependent expression, subcellular localization and association with replication foci: evidence suggesting replication-coupled repair of adenine:8-oxoguanine mispairs, Nucleic Acids Res. 29 (2001) 2802–2809.
[26] Y. Nakabeppu, Regulation of intracellular localization of human MTH1, OGG1, and MYH proteins for repair of oxidative DNA damage, Prog. Nucleic Acid Res. Mol. Biol. 68 (2001) 75–94.
[27] M. Takao, H. Aburatani, K. Kobayashi, A. Yasui, Mitochondrial targeting of human DNA glycosylases for repair of oxidative DNA damage, Nucleic Acids Res. 26 (1998) 2917–2922.
[28] F. Dantzer, L. Luna, M. Bjoras, E. Seeberg, Human OGG1 undergoes serine phosphorylation and associates with the nuclear matrix and mitotic chromatin in vivo, Nucleic Acids Res. 30 (2002) 2349–2357.
[29] K. Nishioka, T. Ohtsubo, H. Oda, T. Fujiwara, D. Kang, K. Sugimachi, Y. Nakabeppu, Expression and differential intracellular localization of two major forms of human 8-oxoguanine DNA glycosylase encoded by alternatively spliced OGG1 mRNAs, Mol. Biol. Cell 10 (1999) 1637–1652.
[30] S. Taladriz, T. Hanke, M.J. Ramiro, M. Garcia-Diaz, M. Garcia De Lacoba, L. Blanco, V. Larraga, Nuclear DNA polymerase beta from *Leishmania infantum* Cloning, molecular analysis and developmental regulation, Nucleic Acids Res. 29 (2001) 3822–3834.
[31] T.T. Saxowsky, G. Choudhary, M.M. Klingbeil, P.T. Englund, *Trypanosoma brucei* has two distinct mitochondrial DNA polymerase beta enzymes, J. Biol. Chem. 278 (2003) 49095–49101.
[32] A. Matsukage, S. Yamamoto, M. Yamaguchi, M. Kusakabe, T. Takahashi, Immunocytochemical localization of chick DNA polymerases alpha and beta +, J. Cell Physiol. 117 (1983) 266–271.
[33] A.W. Plug, C.A. Clairmont, E. Sapi, T. Ashley, J.B. Sweasy, Evidence for a role for DNA polymerase beta in mammalian meiosis, Proc. Natl. Acad. Sci. U.S.A. 94 (1997) 1327–1331.
[34] D.M. Wilson IIIrd, C. Bianchi, Improved immunodetection of nuclear antigens after sodium dodecyl sulfate treatment of formaldehyde-fixed cells, J. Histochem. Cytochem. 47 (1999) 1095–1100.
[35] T.D. Pollard, J.A. Cooper, Actin and actin-binding proteins. A critical evaluation of mechanisms and functions, Annu. Rev. Biochem. 55 (1986) 987–1035.
[36] M. Schliwa, The Cytoskeleton: An Introductory Survey, Springer-Verlag, New York, 1986.
[37] S.L. Rogers, I.S. Tint, P.C. Fanapour, V.I. Gelfand, Regulated bidirectional motility of melanophore pigment granules along microtubules in vitro, Proc. Natl. Acad. Sci. U.S.A. 94 (1997) 3720–3725.
[38] A. Blocker, F.F. Severin, J.K. Burkhardt, J.B. Bingham, H. Yu, J.C. Olivo, T.A. Schroer, A.A. Hyman, G. Griffiths, Molecular requirements for bi-directional movement of phagosomes along microtubules, J. Cell Biol. 137 (1997) 113–129.
[39] G. Bassell, R.H. Singer, mRNA and cytoskeletal filaments, Curr. Opin. Cell Biol. 9 (1997) 109–115.
[40] J.S. Pachter, Association of mRNA with the cytoskeletal framework: its role in the regulation of gene expression, Crit. Rev. Eukaryot. Gene Expr. 2 (1992) 1–18.
[41] R.B. Vallee, G.S. Bloom, W.E. Theurkauf, Micro tubule-associated proteins: subunits of the cytomatrix, J. Cell Biol. 99 (1984) 38s–44s.
[42] J.B. Olmsted, Non-motor microtubule-associated proteins, Curr. Opin. Cell Biol. 3 (1991) 52–58.
[43] T. Sapir, A. Cahana, R. Seger, S. Nekhai, O. Reiner, LIS1 is a microtubule-associated phosphoprotein, Eur. J. Biochem. 265 (1999) 181–188.
[44] R.D. Allen, D.G. Weiss, J.H. Hayden, D.T. Brown, H. Fujiwake, M. Simpson, Gliding movement of and bidirectional transport along single native microtubules from squid axoplasm: evidence for an active role of microtubules in cytoplasmic transport, J. Cell Biol. 100 (1985) 1736–1752.
[45] V. Prahlad, B.T. Helfand, G.M. Langford, R.D. Vale, R.D. Goldman, Fast transport of neurofilament protein along microtubules in squid axoplasm, J. Cell Sci. 113 (Pt 22) (2000) 3939–3946.
[46] P. Giannakakou, D.L. Sackett, Y. Ward, K.R. Webster, M.V. Blagosklonny, T. Fojo, p53 is associated with cellular microtubules and is transported to the nucleus by dynein, Nat. Cell Biol. 2 (2000) 709–717.
[47] B.M. McCartney, M. Peifer, Teaching tumour suppressors new tricks, Nat. Cell Biol. 2 (2000) 58–60.
[48] O.C. Sibon, A. Kelkar, W. Lemstra, W.E. Theurkauf, DNA-replication/DNA-damage-dependent centrosome inactivation in *Drosophila* embryos, Nat. Cell Biol. 2 (2000) 90–95.
[49] V. Bergoglio, M.J. Pillaire, M. Lacroix-Triki, B. Raynaud-Messina, Y. Canitrot, A. Bieth, M. Gares, M. Wright, G. Delsol, L.A. Loeb, C. Cazaux, J.S. Hoffmann, Deregulated DNA polymerase beta induces chromosome instability and tumorigenesis, Cancer Res. 62 (2002) 3511–3514.
[50] H.M. Hut, W. Lemstra, E.H. Blaauw, G.W. Van Cappellen, H.H. Kampinga, O.C. Sibon, Centrosomes split in the presence of impaired DNA integrity during mitosis, Mol. Biol. Cell 14 (2003) 1993–2004.
[51] K.J. Scanlon, M. Kashani-Sabet, L.C. Sowers, Overexpression of DNA replication and repair enzymes in cisplatin-resistant human colon carcinoma HCT8 cells and circumvention by azidothymidine, Cancer Commun. 1 (1989) 269–275.
[52] W.L. Lingle, J.L. Salisbury, Altered centrosome structure is associated with abnormal mitoses in human breast tumors, Am. J. Pathol. 155 (1999) 1941–1951.
[53] C. Lengauer, K.W. Kinzler, B. Vogelstein, Genetic instabilities in human cancers, Nature 396 (1998) 643–649.

[54] G.A. Pihan, A. Purohit, J. Wallace, H. Knecht, B. Woda, P. Quesenberry, S.J. Doxsey, Centrosome defects and genetic instability in malignant tumors, Cancer Res. 58 (1998) 3974–3985.
[55] K.H. Vousden, G.F. Woude, The ins and outs of p53, Nat. Cell Biol. 2 (2000) E178–E180.
[56] K. Conlon, D. Zharkov, M. Berrios, Cell cycle regulation of the murine 8-oxoguanine DNA glycosylase (mOGG1): mOGG1 associates with microtubules during interphase and mitosis, DNA Rep. (Amst.) 3 (2004) 1601–1615.
[57] K.A. Conlon, D.O. Zharkov, M. Berrios, Immunofluorescent localization of the murine 8-oxoguanine DNA glycosylase (mOGG1) in cells growing under normal and nutrient deprivation conditions, DNA Rep. (Amst.) 2 (2003) 1337–1352.
[58] J. Abbotts, D.N. SenGupta, B. Zmudzka, S.G. Widen, V. Notario, S.H. Wilson, Expression of human DNA polymerase beta in *Escherichia coli* and characterization of the recombinant enzyme, Biochemistry 27 (1988) 901–909.
[59] W.A. Beard, S.H. Wilson, Purification and domain-mapping of mammalian DNA polymerase beta, Methods Enzymol. 262 (1995) 98–107.
[60] K.A. Conlon, T. Rosenquist, M. Berrios, Site-directed photochemical disruption of the actin cytoskeleton by actin-binding Rose Bengal-conjugates, J. Photochem. Photobiol. B 68 (2002) 140–146.
[61] K.A. Conlon, M. Berrios, Light-induced proteolysis of myosin heavy chain by Rose Bengal-conjugated antibody complexes, J. Photochem. Photobiol. B 65 (2001) 22–28.
[62] N. Shiina, S. Tsukita, Mutations at phosphorylation sites of Xenopus microtubule-associated protein 4 affect its microtubule-binding ability and chromosome movement during mitosis, Mol. Biol. Cell 10 (1999) 597–608.
[63] M. Katsuki, K. Tokuraku, H. Nakagawa, S. Kotani, Purification and characterization of a new, ubiquitously distributed class of microtubule-associated protein with molecular mass 250 kDa, Eur. J. Biochem. 267 (2000) 7193–7200.
[64] M. Berrios, P.A. Fisher, A myosin heavy-chain-like polypeptide is associated with the nuclear envelope in higher eukaryotic cells, J. Cell Biol. 103 (1986) 711–724.
[65] T. Mitchison, M. Kirschner, Dynamic instability of microtubule growth, Nature 312 (1984) 237–242.
[66] H.L. Nguyen, D. Gruber, J.C. Bulinski, Microtubule-associated protein 4 (MAP4) regulates assembly, protomer-polymer partitioning and synthesis of tubulin in cultured cells, J. Cell Sci. 112 (Pt. 12) (1999) 1813–1824.
[67] M. Moritz, D.A. Agard, Gamma-tubulin complexes and microtubule nucleation, Curr. Opin. Struct. Biol. 11 (2001) 174–181.